Ocean Modelling 116 (2017) 33–47

Contents lists available at ScienceDirect

Ocean Modelling

journal homepage: www.elsevier.com/locate/ocemod

Approximation of wave action flux velocity in strongly sheared mean flows

Saeideh Banihashemi*, James T. Kirby, Zhifei Dong

Center for Applied Coastal Research, University of Delaware, Newark, DE, USA

ARTICLE INFO

Article history:
Received 3 November 2016
Revised 23 May 2017
Accepted 9 June 2017
Available online 10 June 2017

Keywords:
Wave-current interaction
Wave action flux
Ocean models
Waves over sheared currents

ABSTRACT

Spectral wave models based on the wave action equation typically use a theoretical framework based on depth uniform current to account for current effects on waves. In the real world, however, currents often have variations over depth. Several recent studies have made use of a depth-weighted current $\tilde{U}$ due to [Skop, R. A., 1987. Approximate dispersion relation for wave-current interactions. J. Waterway, Port, Coastal, and Ocean Eng. 113, 187–195.] or [Kirby, J. T., Chen, T., 1989. Surface waves on vertically sheared flows: approximate dispersion relations. J. Geophys. Res. 94, 1013–1027.] in order to account for the effect of vertical current shear. Use of the depth-weighted velocity, which is a function of wavenumber (or frequency and direction) has been further simplified in recent applications by only utilizing a weighted current based on the spectral peak wavenumber. These applications do not typically take into account the dependence of $\tilde{U}$ on wave number k, as well as erroneously identifying $\tilde{U}$ as the proper choice for current velocity in the wave action equation. Here, we derive a corrected expression for the current component of the group velocity. We demonstrate its consistency using analytic results for a current with constant vorticity, and numerical results for a measured, strongly-sheared current profile obtained in the Columbia River. The effect of choosing a single value for current velocity based on the peak wave frequency is examined, and we suggest an alternate strategy, involving a Taylor series expansion about the peak frequency, which should significantly extend the range of accuracy of current estimates available to the wave model with minimal additional programming and data transfer.

1. Introduction

Important theoretical advances have been made in the last several decades which have advanced our understanding of wave-current interaction in ocean circulation. Theories have been incorporated in numerical models with the main intent of including wind wave effects in ocean circulation without resolving surface gravity wave motions for computational efficiency. Within typical modeling systems, an ocean circulation model is coupled with a wave generation and propagation model in order to determine wave effects on currents and vice versa. The spectral wave models include the effect of the mean flow in the computation of wave action flux, and the ocean circulation models account for the wave-averaged wave forcing driving or modifying the mean flow.

Spectral wave models are usually based on the theory for waves in the presence of depth-uniform currents. In the real world, however, currents are usually vertically sheared to some degree. Recently, various studies (van der Westhuysen and Lesser, 2007; Ardhuin et al., 2008; Warner et al., 2010) have suggested the use of a depth-weighted current $\tilde{U}(k)$ as the basis for the wave-current interaction in propagation models, where $\tilde{U}(k)$ is the first order correction to the phase speed for an arbitrarily varying current $U(z)$ and is given by

$$\tilde{U}(k) = \frac{2k}{\sinh 2kh} \int_{-h}^{0} U(z) \cosh 2k(h+z)\, dz \tag{1}$$

where h is the water depth and k is the wave number (Skop, 1987; Kirby and Chen, 1989). In application, this approach is often further truncated by using $\tilde{U}(k_p)$ as the representative value of $\tilde{U}$ for all wave components, where k_p denotes the wavenumber at the spectral peak frequency. This procedure is now included as an option in widely used models such as Delft-3D and COAWST (Elias et al., 2012; Kumar et al., 2011; 2012). We remark here that the perturbation scheme of Kirby and Chen (1989), defined originally for the case of weak current, can be straightforwardly modified to cover the case of a strong current with weak additional shear. Assuming a fairly arbitrary split between a depth uniform and depth varying current

$$U(z) = U_0 + \alpha U_1(z); \qquad \alpha \ll 1 \tag{2}$$

* Corresponding author.
E-mail addresses: bhashemi@udel.edu, s.banihash@gmail.com (S. Banihashemi).

http://dx.doi.org/10.1016/j.ocemod.2017.06.002
1463-5003/

and repeating the procedure used to develop the solution in Kirby and Chen quickly establishes that the choice for leading order current speed is $U_0 = \tilde{U}$, with the details of the overall solution maintained up to second order. The parameter α represents the magnitude of current shear; a scaling analysis based on finite depth waves with horizontal and vertical length scales proportional to k^{-1}, leads naturally to an expression

$$\alpha = \frac{\Omega}{kU_s} \tag{3}$$

where Ω characterizes the maximum value of shear in the current profile, and U_s is the surface current speed. The expressions developed in both the perturbation solution and the analytic solution for constant shear discussed below are both easier to interpret using a slightly different expression

$$\alpha = \frac{\Omega h}{U_s} \tag{4}$$

which is used throughout the remainder of the paper.

The purpose of this study is to demonstrate the inappropriet-ness of the use of the weighted current $\tilde{U}$ as the current component of the group velocity, and to examine the effect of using either the correct or incorrect estimate of the current speed evaluated only at the spectral peak frequency. We evaluate the accuracy of approximate solutions in comparison to analytical or numerical solutions for the full theory based on the Rayleigh stability equation. The theory described here is limited to unidirectional propagation on a following or opposing current, and so currents and wave numbers appear as scalars rather than vectors. In Section 2, the problem for a linear wave in a uniform domain with arbitrary current $U(z)$ is established. We then outline the common approximations for group velocity used in modeling and the errors resulting in these applications. In Section 3, we evaluate the approximations for the analytic case of a wave on a current with constant vorticity, and establish the consistency of the expressions for group velocity derived from the perturbation solution of Kirby and Chen (1989). Section 4 examines comparable results of the numerical solution for a current profile measured at the mouth of the Columbia River (MCR) (Kilcher and Nash, 2010). In Section 5, we evaluate the shortcomings of practical approximations in existing coupled circulation-spectral wave models, where it is typical to use only $\tilde{U}(k_p)$ as the current speed. Finally, in Section 6 we describe a strategy for providing a compact but significantly more accurate representation of current advection velocity in SWAN or similar models, using a Taylor series expansion of the expression for the wavenumber-dependent current speed about the reference value at the peak frequency.

2. Theory and approximate expressions for the absolute group velocity C_{ga}

2.1. General theory

We consider the linearized wave motion of an incompressible, inviscid fluid, with wave number $\mathbf{k}$ and phase velocity $\mathbf{C_a} = \omega\mathbf{k}/k^2$, propagating on a stream of velocity $\mathbf{U}(z)$ in finite water depth h. Current and depth variables are assumed to be uniform in horizontal directions (Fig. 1). ω denotes the absolute wave frequency in a stationary frame of reference, which also fixes the value of $\mathbf{U}(z)$. We seek solutions for the vertical component of the wave orbital velocity

$$w(\mathbf{x}, z, t) = \tilde{w}(z)e^{i(\mathbf{k}\cdot\mathbf{x}-\omega t)} \tag{5}$$

The problem for the vertical structure of plane waves in a spatially uniform domain, riding on a vertically sheared current $\mathbf{U}(z)$, is then given by an extension of the Rayleigh equation to allow for

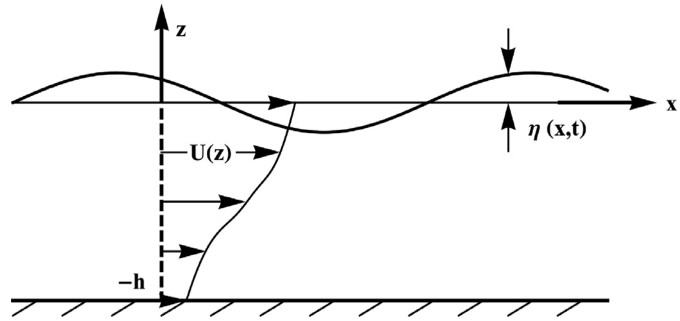

Fig. 1. Definition sketch.

an oblique angle between wave and current direction as well as possible rotation of the current vector over depth

$$\begin{aligned} \sigma(z)(\tilde{w}'' - k^2\tilde{w}) - \sigma''(z)\tilde{w} = 0; &\qquad -h \le z \le 0 \\ \sigma_s^2\tilde{w}' - [gk^2 + \sigma_s\sigma']\tilde{w} = 0; &\qquad z = 0 \\ \tilde{w} = 0; &\qquad z = -h \end{aligned} \tag{6}$$

where primes denote differentiation with respect to z and g is the gravitational constant. The quantity $\sigma(z) = \omega - \mathbf{k}\cdot\mathbf{U}(z)$ represents a depth-varying relative frequency, with σ_s denoting the value at the mean surface $z = 0$. The separate use of the kinematic surface boundary condition for a surface wave of form $\eta = a\exp i(\mathbf{k}\cdot\mathbf{x} - \omega\mathbf{t})$ gives $\tilde{w}(0) = -i\sigma_s a$.

The model (6) has been used in a number of studies of arbitrary or idealized velocity distributions; see reviews by Peregrine (1976), Jonsson (1990) and Thomas and Klopman (1997). For the general case of arbitrary $U(z)$, Voronovich (1976) has described the conservation law, in the geometric optics approximation, for an adiabatic invariant corresponding to the wave action density. Evaluation of these results requires knowledge of a solution to (6), however. Karageorgis (2012) has shown a method for constructing expressions for the dispersion relation for waves on a number of vertical vorticity distributions, but does not consider the further determination of the group velocity.

For the case of weak shear, solutions to (6) may be obtained using a perturbation approach, described to leading order for deep water by Stewart and Joy (1974) and extended to finite depth by Skop (1987) and to second order by Kirby and Chen (1989). Considering deep water waves, Shrira (1993) has further demonstrated how series solutions may be extended to high order. Alternately, numerical solutions may be obtained using a shooting method due to Fenton (1973). In the following, we limit ourselves to the evaluation of the first and second-order solutions presented in Kirby and Chen (1989) and further limit ourselves to waves and currents propagating in the same direction. For definiteness, we suppose that waves are propagating towards the right with $c > 0$ and $k > 0$, while the current can be propagating in either $\pm\, x$ direction.

2.2. Perturbation solution of Kirby and Chen (1989)

Following Kirby and Chen (1989), we assume that the steady current velocity is small relative to some measure of wave phase speed. Here, we use a Froude number based on the surface velocity $U_s = U(0)$ defined by

$$F = \frac{U_s}{\sqrt{gh}}; \qquad |F| \ll 1 \tag{7}$$

The wave phase speed is given by

$$C_a = \frac{\omega}{k} = C_0 + (F)C_1 + (F^2)C_2 + O(F^3) \tag{8}$$

where we indicate ordering w/r F schematically and retain dimensional expressions for now. C_0 is the usual result for linear waves on a stationary water column, and is given by

$$C_0 = \sqrt{\frac{g}{k}\tanh kh} \tag{9}$$

C_1 and C_2 arise from the current-induced Doppler shift, with $C_1 = \tilde{U}$ in (1) and C_2 given by

$$\begin{aligned} C_2 = & \frac{\tilde{U}}{2C_0}[4kI_1(0) - (1 + 2\cosh 2kh)\tilde{U}] \\ & + \frac{k^2C_0}{2gf_0^2(0)}\int_{-h}^{0} U^2(z)[1 + 2\cosh^2 k(h+z)]\,dz \\ & + \frac{2k^3C_0}{gf_0^2(0)}\int_{-h}^{0}[I_2(z)I_1'(z) - I_1(z)I_2'(z)]\,dz \end{aligned} \tag{10}$$

with

$$\begin{aligned} I_1(z) &= \int_{-h}^{z} U(\xi)\sinh 2k(h+\xi)\,d\xi \\ I_2(z) &= \int_{-h}^{z} U(\xi)\cosh 2k(h+\xi)\,d\xi \\ f_0 &= \sinh k(h+z) \end{aligned} \tag{11}$$

To $O(F^2)$, the absolute wave group velocity $\tilde{C}_{ga}$ determined from the perturbation solution is given by

$$\tilde{C}_{ga} = \frac{\partial\omega}{\partial k} = \frac{\partial(kC_a)}{\partial k} = \frac{\partial(kC_0)}{\partial k} + (F)\frac{\partial(k\tilde{U})}{\partial k} + (F^2)\frac{\partial(kC_2)}{\partial k} \tag{12}$$

The first, $O(F^0)$ term on the right hand side is the usual expression for the current-free case, given by

$$C_{g0} = \frac{C_0}{2}(1+G); \qquad G = \frac{2kh}{\sinh 2kh} \tag{13}$$

The second component on the RHS of (12) gives the expression

$$\begin{aligned} \hat{U} &= \tilde{U} + k\frac{\partial\tilde{U}}{\partial k} = (2 - G\cosh 2kh)\tilde{U} \\ & + \frac{4k^2}{\sinh 2kh}\int_{-h}^{0}(h+z)U(z)\sinh 2k(h+z)\,dz \end{aligned} \tag{14}$$

which clearly differs from the apparent phase speed correction $\tilde{U}$ at $O(F)$. The remaining term at $O(F^2)$ is derived in sections 3 and 4 for the specific cases studied here.

It is clear that the expression

$$C_{ga} = C_{g0} + \tilde{U} \tag{15}$$

suggested for use by a number of authors, does not represent a consistent approximation for the current component of the group velocity at $O(F)$. This point was made in the original study of Kirby and Chen (1989), and we re-examine that conclusion in the context of two cases in Sections 3 and 4. The result that $\hat{U}$ rather than $\tilde{U}$ is the correct leading-order estimate of current velocity for use in the wave action equation is the first main point of this study.

In the following sections, the validity of the first and second order perturbation approximation will be examined for two cases; (1) a linear shear current, where the analytical dispersion relation has been obtained from the Rayleigh equation by Thompson (1949), and (2) a current profile measured at the mouth of the Columbia River (Kilcher and Nash, 2010), where a numerical solution is found using a shooting method described in Dong and Kirby (2012).

3. Wave on a current with constant shear

The linear problem for waves riding on a horizontally-uniform current with constant vertical shear has an exact solution. For the case of co-linear wave and current flow, the wave motion is described by a potential, and no vorticity is developed at the wave frequency (Thompson, 1949). Maïssa et al. (2016) examine the resulting expressions for group velocity in the co-linear case without and with surface tension, and consider blocking conditions for waves on an opposing stream, corresponding to the limit $C_{ga} \to 0$. For the case of waves propagating at an angle to the current direction, Constantin (2011) and others have shown that a flow with constant vorticity and irrotational wave motion does not exist. Ellingsen (2016) points out that this result simply implies that the waves are then described by a rotational flow with vorticity fluctuating at wave frequency. The resulting problem is completely described by (6) with additional work needed to develop an expression for the vorticity. Ellingsen (2016) considers the case of deep water and develops expressions for the resulting horizontal vorticity; the extension to finite water depth is described by Dong (2016); see section 3.1.2.

We limit attention here to the co-linear case and let

$$U(z) = U_s + \Omega z = U_s(1 + \alpha\frac{z}{h}) \tag{16}$$

where U_s is the surface velocity, Ω is the constant current shear and α is the current shear parameter defined in (4). The exact dispersion relation, written in terms of the phase speed relative to surface velocity $C_{rs} = C_a - U_s$, is given by (Thompson, 1949)

$$C_{rs}^2 = (gh - \alpha U_s C_{rs})\frac{\tanh kh}{kh} \tag{17}$$

The exact expression for the absolute group velocity $C_{ga}^e = \partial\omega/\partial k$ is found from (17) to be

$$C_{ga}^e = U_s + \left(\frac{g(1+G) - (\alpha U_s/h)C_{rs}G}{2g - (\alpha U_s/h)C_{rs}}\right)C_{rs} \tag{18}$$

Introducing the Froude number $F = U_s/\sqrt{gh}$, we normalize the group velocity and phase speed by $(gh)^{1/2}$ and obtain

$$\frac{C_{ga}^e}{\sqrt{gh}} = C_{ga}^{e*} = F + \frac{(1+G) - \alpha FGC_{rs}^*}{2 - \alpha FC_{rs}^*}C_{rs}^* \tag{19}$$

where $C_{rs}^* = C_{rs}/\sqrt{gh}$. Using (17) leads to

$$C_{rs}^* = \frac{1}{2}(\sqrt{4\mu + \alpha^2F^2\mu^2} - \alpha\mu F) \tag{20}$$

with μ defined as

$$\mu = \frac{\tanh kh}{kh} \tag{21}$$

Turning to the perturbation solution of Kirby and Chen (1989), we obtain results to $O(F^2)$ and compare them to the full solution to determine their range of validity. The dimensionless $O(1)$ phase speed and group velocity are given by

$$C_0^* = \sqrt{\mu}; \qquad C_{g0}^* = \frac{1}{2}\sqrt{\mu}(1+G) \tag{22}$$

At $O(F)$, the depth weighted current $\tilde{U}$ and it's derivative with respect to k are given in dimensionless form by

$$\tilde{U}^* = \frac{\tilde{U}}{\sqrt{gh}} = F(1 - \alpha\frac{\mu}{2}); \qquad \frac{\partial\tilde{U}^*}{\partial k} = \alpha\frac{F}{2}\frac{\mu}{k}(1-G) \tag{23}$$

giving a leading order current contribution to the group velocity

$$\hat{U}^* = \frac{\hat{U}}{\sqrt{gh}} = F\left(1 - \frac{1}{2}\alpha\mu G\right) \tag{24}$$

Finally, at $O(F^2)$, the correction to the phase speed is given by

$$C_2^* = \frac{1}{8}\alpha^2F^2\mu^{3/2} \tag{25}$$

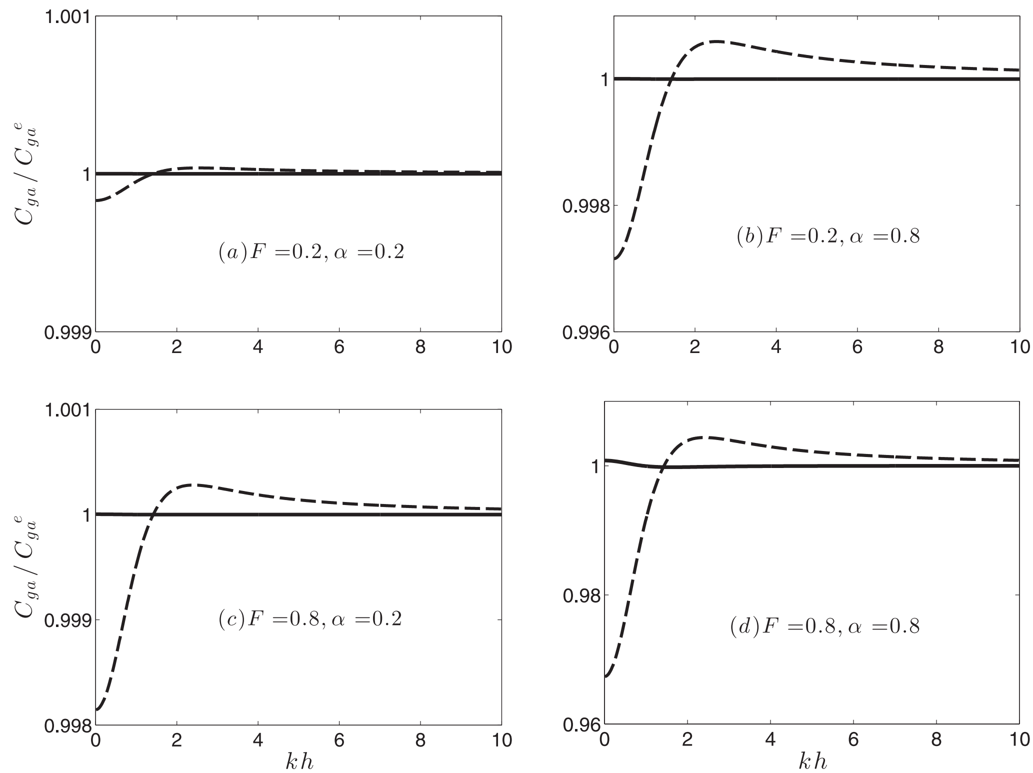

Fig. 2. Wave group velocity comparison C_{ga}/C^e_{ga} vs relative depth kh: linear shear current. Solid lines indicate $O(F^2)$ approximation; dashed lines indicate $O(F)$ approximation.

The $O(F^2)$ correction to the group velocity is then

$$C^*_{g2} = \frac{1}{\sqrt{gh}}\frac{\partial(kC_2)}{\partial k} = \frac{1}{16}F^2\alpha^2\mu^{3/2}(3G-1) \tag{26}$$

The results for the complete expressions for group velocity are collected here for convenience:

$$\text{Exact} \qquad C^{e*}_{ga} = F + \frac{(1+G) - \alpha F G C^*_{rs}}{2 - \alpha F C^*_{rs}} C^*_{rs} \tag{27a}$$

$$O(F) \qquad \tilde{C}^*_{ga} = \frac{1}{2}\sqrt{\mu}(1+G) + F\left(1 - \frac{1}{2}\alpha\mu G\right) \tag{27b}$$

$$O(F^2) \qquad \tilde{C}^*_{ga} = \frac{1}{2}\sqrt{\mu}(1+G) + F\left(1 - \frac{1}{2}\alpha\mu G\right) + \frac{1}{16}F^2\alpha^2\mu^{3/2}(3G-1) \tag{27c}$$

It may be verified after some tedious algebra that the resulting expression $\tilde{C}^*_{ga}$ agrees with the expansion of the exact result (27a) truncated at either $O(F)$ or $O(F^2)$ as desired. The perturbation solution is thus consistent with the full solution to the order considered, with a clear indication that the commonly used $\tilde{U}$ is not the correct advection velocity to use in the wave action equation.

3.1. Following currents F > 0

The results for the first and second order perturbation solutions expressed in (27) are compared to the full theory in Fig. 2 for various choices of α and for $F > 0$, corresponding to currents flowing in the direction of wave propagation. (Values of $0 \le |F| \le 1$ and $0 \le \alpha \le 1$ represent variation from weak to strong current and weak to strong shear, respectively. The values here are chosen purely for example). Both the first and second order perturbation solutions are quite good approximations to the full solution, with little indication that there is a need to use the $O(F^2)$ correction in practice.

Fig. 3 compares the first order approximations $\tilde{U}^*$ and $\hat{U}^*$ to the second order correction $(\hat{U}^* + C^*_{g2})$ for various choices of α and F. It can be seen that, as the current becomes more sheared, the error of neglecting the term $k\partial\tilde{U}/\partial k$ increases.

3.2. Opposing currents F < 0 and blocking

For the case of an opposing current with $F < 0$, the group velocity of the wave train is decreased by the current. When the current becomes strong enough to reduce the group velocity to zero (or $C_{ga} \to 0$), wave blocking occurs and waves are unable to transport energy in the direction of propagation. Results for the case of constant shear are discussed in Maïssa et al. (2016). We investigate the validity of the perturbation solution in predicting the blocking current speed by setting the absolute group velocity to zero in each expression in (27). Using the exact expression (27a), we obtain the following nonlinear equation for blocking of waves

$$F^2(\alpha C^*{}_{rs}) + F\left(\alpha G C^{*\,2}_{rs} - 2\right) - (1+G)C^*_{rs} = 0 \tag{28}$$

which is solved numerically in MATLAB. The long wave limit for the exact solution is given by

$$kh \to 0: \qquad F_b = \frac{-1}{(1-\alpha)^{1/2}} \tag{29}$$

which is singular for $\alpha = 1$, where the current speed is reduced to zero at the bottom. This singularity results from the linearization of the problem with respect to the wave motions. A more complete examination of the critical Froude number F_c in a hydraulic flow with constant vertical shear yields the result $F_c = -1/(1-\alpha+\alpha^2/12)^{1/2}$, where criticality corresponds to blocking of upstream propagation of information by infinitesimal waves.) The $O(F)$ approximation, obtained from (27b), is given by

$$F_b = \frac{\mu^{1/2}(1+G)}{(\alpha\mu G - 2)} \tag{30}$$

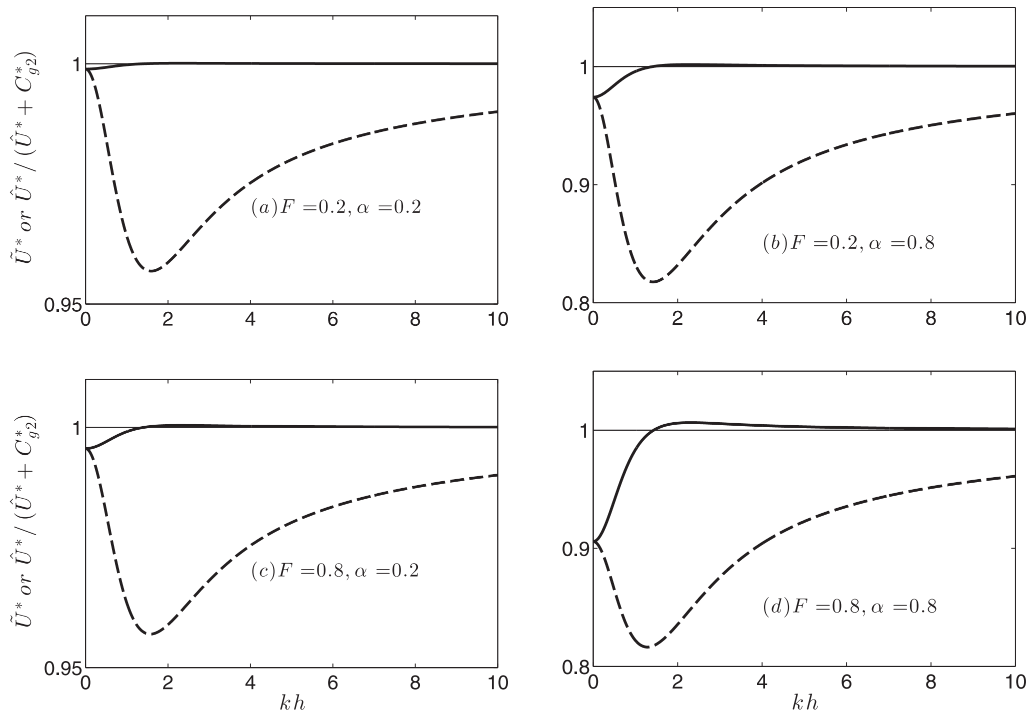

Fig. 3. Ratio of first order approximations $\tilde{U}$ and $\hat{U}$ to the second order correction $(\hat{U}^* + C^*_{g2})$ for various choices of current shear α and Froude number F. Solid lines are for the consistent $O(F)$ contribution $\hat{U}^*$, while dashed lines are for the depth weighted current $\tilde{U}^*$, used inconsistently as the current component of the group velocity.

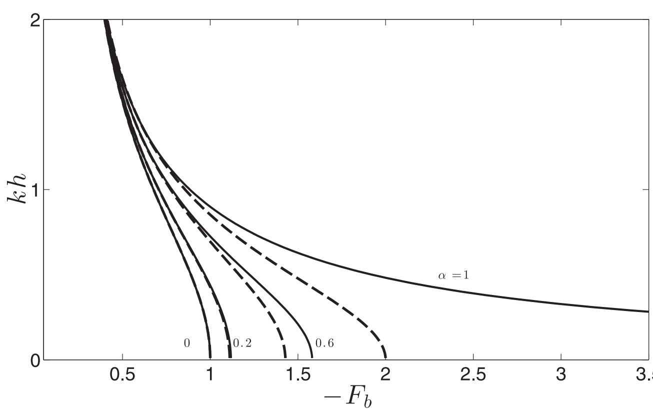

Fig. 4. Blocking current Froude number vs corresponding relative depth kh for various choices of current shear α. (Solid lines) exact solution, (dashed lines) $O(F)$ approximation.

with long wave asymptote $F_b = -1/(1 - \alpha/2)$. This long wave limit is a valid leading order estimate for the exact result (29) only in the limit of small shear α; the source of this additional restriction is not immediately clear in the context of the small F restriction in the perturbation solution. It is noted that a re-ordering of the problem (6) to allow for $O(1)$ current speeds but with a small shear restriction recovers the same perturbation series to the order given here, and thus the small shear limitation is perhaps a better interpretation in the context of the large F values associated with blocking.

Results for the first order approximation are shown in Fig. 4 in comparison to the full theory. Exact and $O(F)$ approximate solutions for the blocking current speed show significant deviations for values of $kh < 1$. For small values of α, (30) may be approximated by $F_b = -1/(1 - \alpha/2)$, in agreement with the perturbation solution.

At $O(F^2)$, solving the quadratic equation for F_b resulting from (27c) gives the expression

$$F_b = \frac{-B + [B^2 - 4AC]^{1/2}}{2A} \tag{31}$$

with

$$A = \alpha^2 \mu^{3/2}(3G - 1); \quad B = 16\left(1 - \frac{1}{2}\alpha\mu G\right); \quad C = 8\mu^{1/2}(1 + G) \tag{32}$$

Real-valued solutions for F_b only exist for positive values of the discriminant $B^2 - 4AC$. Since μ and G are both functions of kh, it is simpler to solve the equation $B^2 = 4AC$ for a critical shear α_c as a function of kh; doing so gives

$$\alpha_c = \frac{4\left[\left(\frac{3}{2}G^2 - G - \frac{1}{2}\right)^{1/2} - G\right]}{\mu\left(G^2 + 2G - 1\right)} \tag{33}$$

Using (33) in (31) then gives a critical blocking Froude number F_{bc} for each kh, given by

$$F_{bc} = \frac{-B}{2A} = -\frac{8\left(1 - \frac{1}{2}\alpha_c\mu G\right)}{\alpha_c^2 \mu^{3/2}(3G - 1)} \tag{34}$$

with the $O(F^2)$ solution for blocking breaking down for $\alpha > \alpha_c$ at each kh. The long wave results are given by

$$kh \to 0: \quad \alpha_c = 2(\sqrt{2} - 1) \approx 0.828; \quad F_{bc} = -(2 + \sqrt{2}) \approx -3.414 \tag{35}$$

with the solution breaking down at smaller current speeds with increasing kh and α, as indicated by the dash-dot curve in Fig. 5.

Fig. 6 compares the first and second order perturbation solutions to the exact solution for various choices of $F < 0$ and α. The solutions are compared for a range of kh values corresponding to unblocked waves range before the waves are blocked by the current. Both first and second order perturbation solutions are accurate predictors of group velocity for current speeds up to the blocking condition when shear α is small; however, as indicated above,

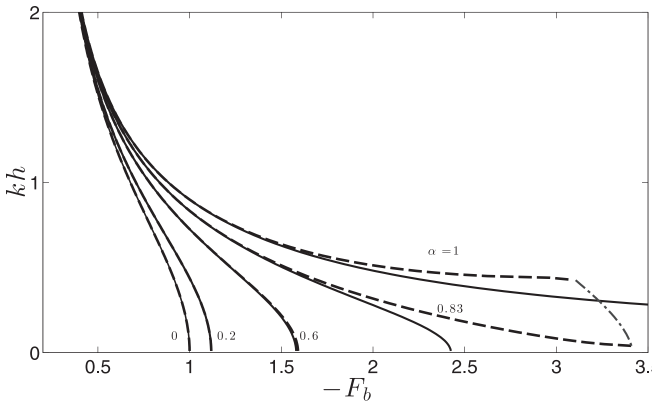

Fig. 5. Blocking current Froude number F_b vs corresponding relative depth kh for various choices of current shear α. Solid lines show the exact solution, dashed lines are the $O(F^2)$ approximation. The dash-dot line shows the locus of F_{bc} values where the second order solution breaks down, as indicated in (34).

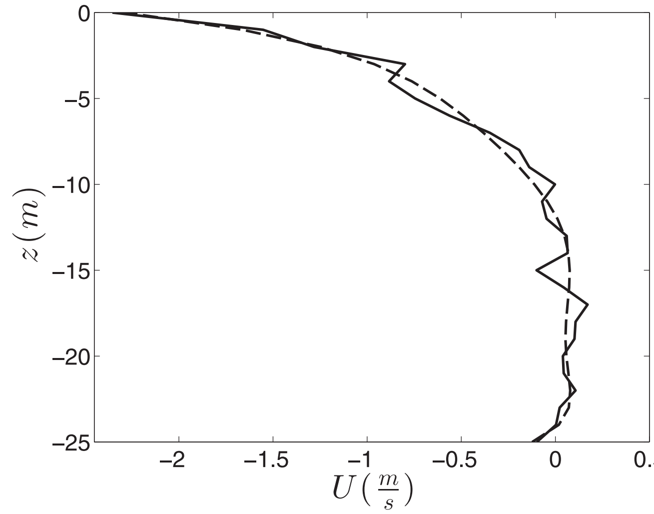

Fig. 7. Columbia River current profile during ebb tide. Solid line is measured data (Kilcher and Nash, 2010) and the dashed line is a 6th order polynomial fit to the data.

the approximations become weak for long waves and values of dimensionless shear much in excess of $\alpha = 0.5$.

4. Columbia river velocity profile

In this section we compare the group velocities obtained from different approximations using a measured current profile from the mouth of the Columbia River (MCR). The Columbia River is well known for it's large freshwater discharge and the resulting development of a rapidly moving, buoyant plume during ebb tide conditions. Here, we select a sample velocity profile collected by a pole-mounted ADCP during the RISE (River Influences on Shelf Ecosystems) project (Kilcher and Nash, 2010). The profile, shown in Fig. 7, represents a maximum ebb condition for the time frame covered by the file. The normalized shear parameter for this current profile is $\alpha \sim 8$ which indicates a strongly sheared current. We consider the idealized case of wave propagating landward against the opposing current at Columbia river mouth. We follow a general procedure of fitting polynomials to either measured profiles or profiles taken from gridded model results in order to establish a basis for computing weighted current values. Expressions below are based

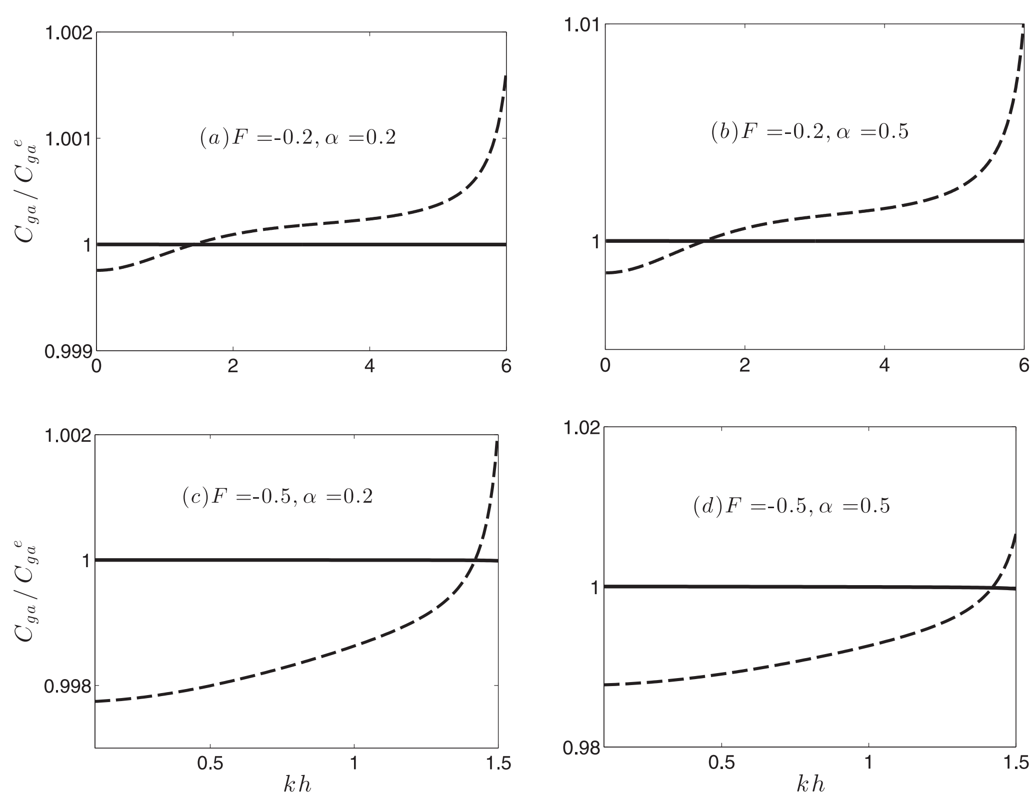

Fig. 6. Wave group velocity comparison C_{ga}/C_{ga}^e vs relative depth kh for various choices of current shear α and Froude number F. Solid lines are $O(F^2)$ approximation and dashed lines are the $O(F)$ approximation.

on the form

$$U(z) = U_s \sum_{n=0}^{N} a_n \left(\frac{z}{h}\right)^n \tag{36}$$

with current speed referenced to the surface value U_s and with dimensionless a_n's. The relative depth is assumed to be varying between $kh \sim 0.5$ to $kh \sim 3$. Calculations here are carried out using $N = 6$, with the fitted profile for the demonstration case also shown in Fig. 7. Results for expressions for $\tilde{U}$, $\hat{U}$, C_2 and C_{g2} resulting from evaluating the perturbation solutions after introducing the expansion (36) are presented in Appendix A.

4.1. Numerical solution

In the absence of an analytic solution for the original problem (6), a numerical method is used to solve the Rayleigh equation. We first introduce normalized vertical shape functions $L(z) = \sigma(z)/\sigma_s$ for the relative frequency and $f(z) = \tilde{w}/(-i\sigma_s a)$, where a is wave amplitude. (6) becomes

$$\begin{aligned} f'' - (k^2 + \frac{L''}{L})f &= 0; \qquad -h \le z \le 0 \\ f &= 0; \qquad z = -h \\ f' &= (L' + \frac{gk^2}{\sigma_s^2})f; \qquad z = 0 \end{aligned} \tag{37}$$

We then introduce a non-dimensional vertical coordinate $\hat{z} = z/h$ following Fenton (1973) and define a new dependent variable

$$Q(\hat{z}) = \frac{f}{hf'} \tag{38}$$

The problem is then reduced to a Riccati equation

$$\begin{aligned} \frac{dQ}{d\hat{z}} &= 1 - \gamma^2 Q^2; \qquad -1 \le \hat{z} \le 0; \\ \gamma^2(\hat{z}) &= (kh)^2 + \frac{L''}{L} \\ Q &= \frac{\sigma_s^2}{(gk^2h + L'\sigma_s^2)}; \qquad \hat{z} = 0; \\ Q &= 0; \qquad \hat{z} = -1 \end{aligned} \tag{39}$$

The Riccati equation is solved using a shooting method (Fenton, 1973; Kirby and Chen, 1989; Dong and Kirby, 2012), with the absolute frequency ω determined from the value of $Q(0)$. We then calculate the derivative of the absolute frequency w/r k using a central difference method to evaluate the group velocity C_{ga}^n numerically.

$$C_{ga}^n = \frac{\partial \omega}{\partial k} \approx \frac{\omega(k + \Delta k) - \omega(k - \Delta k)}{2\Delta k} \tag{40}$$

4.2. Comparison of numerical and perturbation results

Using the expressions in Appendix A, group velocity comparisons based on first and second order perturbation approximations are shown in Fig. 8. The perturbation solutions are seen to be fairly good approximations. Fig. 9 compares the incorrect first order approximation $\tilde{U}$ and the consistent first order approximation $\hat{U}$ to the second order correction $(\hat{U} + C_{g2})$. The neglected term $k\partial\tilde{U}/\partial k$ is shown to be as big as 40% of the second order perturbation correction, indicating the magnitude of the error involved in using $\tilde{U}$ instead of $\hat{U}$ as the estimate for current velocity in the wave model. At the same time, $\hat{U}$ provides a fairly accurate estimate of the current component of the group velocity when compared to the higher order $O(F^2)$ result.

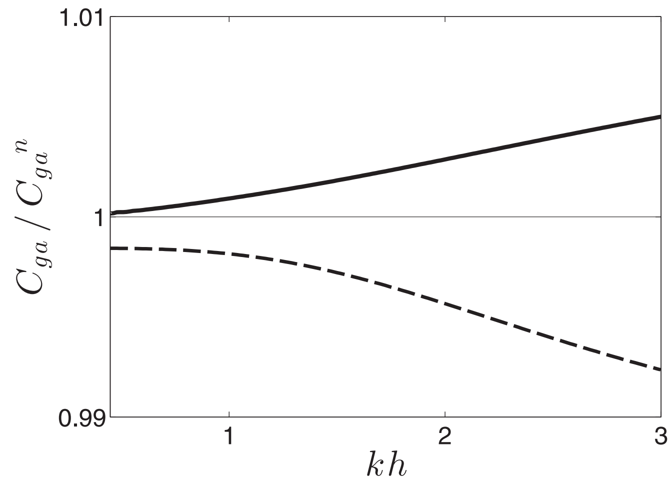

Fig. 8. Wave group velocity comparison $C_{ga}/C_{ga}{}^n$ vs relative depth kh: Mouth of Columbia River (MCR). Solid line indicates $O(F^2)$ approximation and dashed line indicates $O(F)$ approximation.

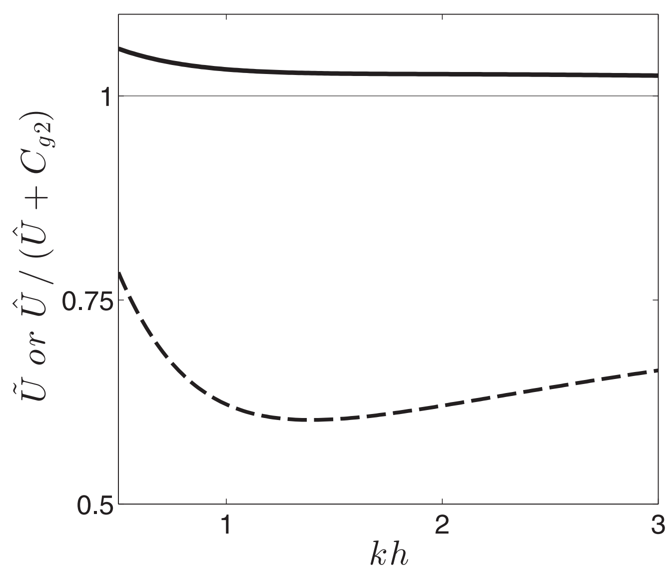

Fig. 9. Ratio of first order approximations $\tilde{U}$ and $\hat{U}$ to the second order correction $(\hat{U} + C_{g2})$: Mouth of Columbia River (MCR). Solid line is $\hat{U}$ and dashed line is $\tilde{U}$.

5. Common approximations in modeling

Choices for current values to be used in evaluating current effects on waves have historically included depth-averaged current $\overline{U}$ or surface current U_s. More recently, as discussed above, several investigators have suggested using the depth-weighted current $\tilde{U}$ as the choice for effective current (van der Westhuysen and Lesser, 2007; Ardhuin et al., 2008; Warner et al., 2010). Lesser (2009) introduced the procedure of using a single value $\tilde{U}(k_p)$ instead of the frequency dependent $\tilde{U}(k)$ to represent the current used for all frequency-directional components, where k_p is the wavenumber at peak frequency; this procedure is included as an option in Delft-3D (Lesser, 2009); see also discussions in Elias et al. (2012). The approach has also been introduced in ROMS (Warner et al., 2010).

As has been mentioned above, direct use of $\tilde{U}$ as a replacement for depth averaged velocity incurs an error of $O(F)$ in action flux conservation. In this section, we examine the limitations of these approximations for both the analytic and numerical cases considered above. We also consider a fourth choice of $\hat{U}(k_p)$, the correct estimate of the advective current component to $O(F)$, but

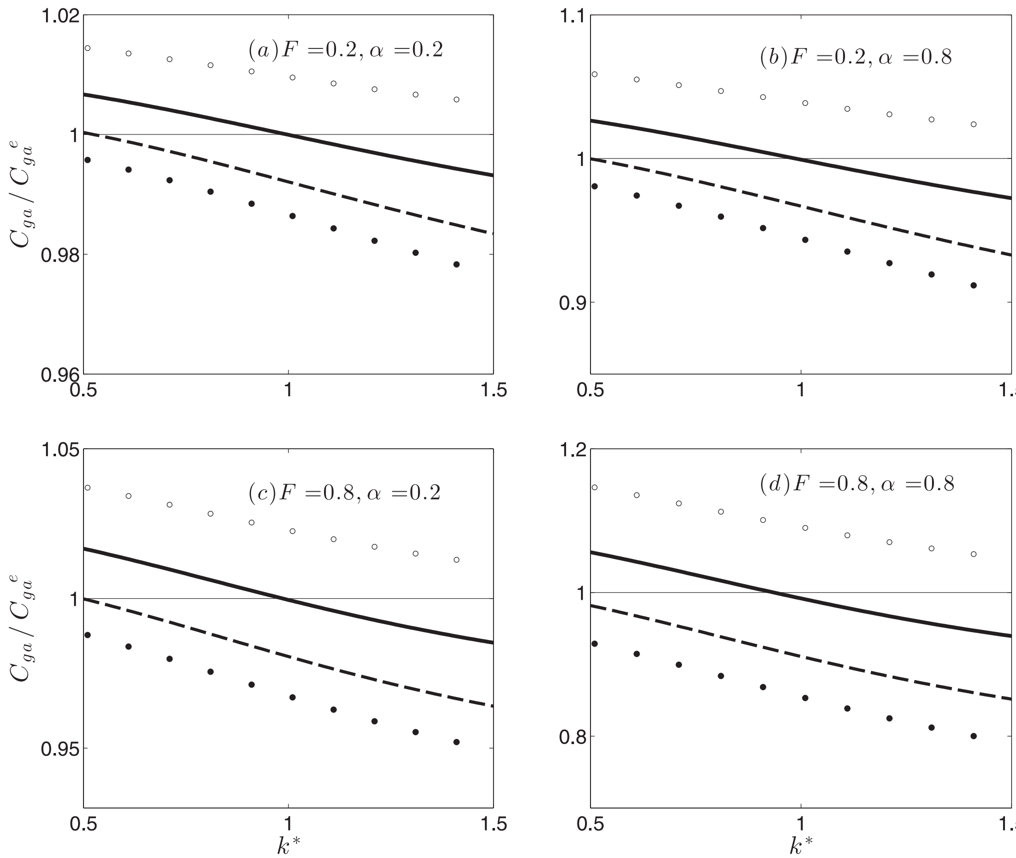

Fig. 10. Wave group velocity comparison C_{ga}/C_{ga}^{e} vs normalized wave number $k^* = k/k_p$, with $k_p h = 1$: linear shear flow. Solid lines are using $\hat{U}(k_p)$, dashed lines are based on $\tilde{U}(k_p)$, dots indicate the depth averaged approximation and the circles are only using the surface value U_s.

evaluated only at the peak frequency. We assume that the spectrum is narrow banded in the sense that $|k-k_p|/k_p \ll 1$ for any k within the energetic part of the spectrum and also select three peak wave numbers corresponding to $k_p h = 1, 2$ and 3. Figs. 10–12, and compare the validity of these approximations for the linear shear current, while Figs. 13–15, and show the same comparison for the MCR current profile. It can be seen that although the depth weighted current $\tilde{U}(k_p)$ gives a better approximation compared to the choice of depth-average or surface current, the effect of neglecting the term $k\partial\tilde{U}/\partial k$ can still cause significant errors even at the peak frequency. It should also be noted that, despite the fact that $\hat{U}(k_p)$ is a more fundamentally accurate choice near the spectral peak, it still produces a comparable rate of deviation between modeled and true group velocity estimates with increasing Δk. This would indicate the potential need to represent frequency dependence in $\hat{U}$ in applications to broad-banded frequency spectra, unless a more advantageous strategy can be developed using values computed at the peak frequency alone. We explore such an extension in the following section.

6. An improved approximation based on taylor expansion about k_p

The comparisons of the group velocity approximations in previous sections have indicated that significant errors may be incurred by neglecting either the contribution of the term $k\partial\tilde{U}/\partial k$ to the group velocity at $O(F)$ or the wavenumber dependence of $\hat{U}$. For the remainder of this discussion, it should be clear that we advocate the use of the velocity $\hat{U}$ in place of $\tilde{U}$ in any coupled wave-current modeling system. In this section, we describe a possible strategy for additionally recovering wavenumber dependence in $\hat{U}$ using only values calculated at the peak wavenumber k_p, thereby minimizing the amount of additional information to be passed from the circulation model to the wave model.

The Taylor expansion of $\hat{U}(k)$ about the peak wavenumber k_p is given to leading order by

$$\hat{U}(k) = \hat{U}(k_p) + \frac{d\hat{U}}{dk}\Big|_{k_p}(\Delta k) + O(\Delta k^2) \tag{41}$$

$$\Delta k = k - k_p \tag{42}$$

Using the relation between $\hat{U}$ and $\tilde{U}$ indicated in (14), we obtain

$$\begin{aligned}\hat{U}(k) &= \tilde{U}(k_p)+k_p\frac{\partial\tilde{U}}{\partial k}\Big|_{k_p} + \Delta k\left[\frac{\partial\tilde{U}}{\partial k}\Big|_{k_p} + \frac{\partial\tilde{U}}{\partial k}\Big|_{k_p} + k\frac{\partial^2\tilde{U}}{\partial k^2}\Big|_{k_p}\right] + O(\Delta k)^2 \\ &= \tilde{U}(k_p) + \frac{\partial\tilde{U}}{\partial k}\Big|_{k_p}[2k-k_p] + k_p\frac{\partial^2\tilde{U}}{\partial k^2}\Big|_{k_p}\Delta k + O(\Delta k)^2\end{aligned} \tag{43}$$

To $O(\Delta k)$, the group velocity is then given by

$$C_{ga} = \frac{C_0}{2}(1+G) + \hat{U}(k) \tag{44}$$

This procedure retains the effect of the wavenumber dependence of $\tilde{U}$ but requires the passage of only one or two additional coefficients to the wave model, depending on whether expressions based on $\hat{U}$ or $\tilde{U}$ are employed. The extra data can then be used in the wave model to compute frequency and direction-dependent current values for use with each component wave.

The accuracy of the approximation is compared to prediction of group velocity using $\hat{U}(k)$ evaluated only at the peak wavenumber

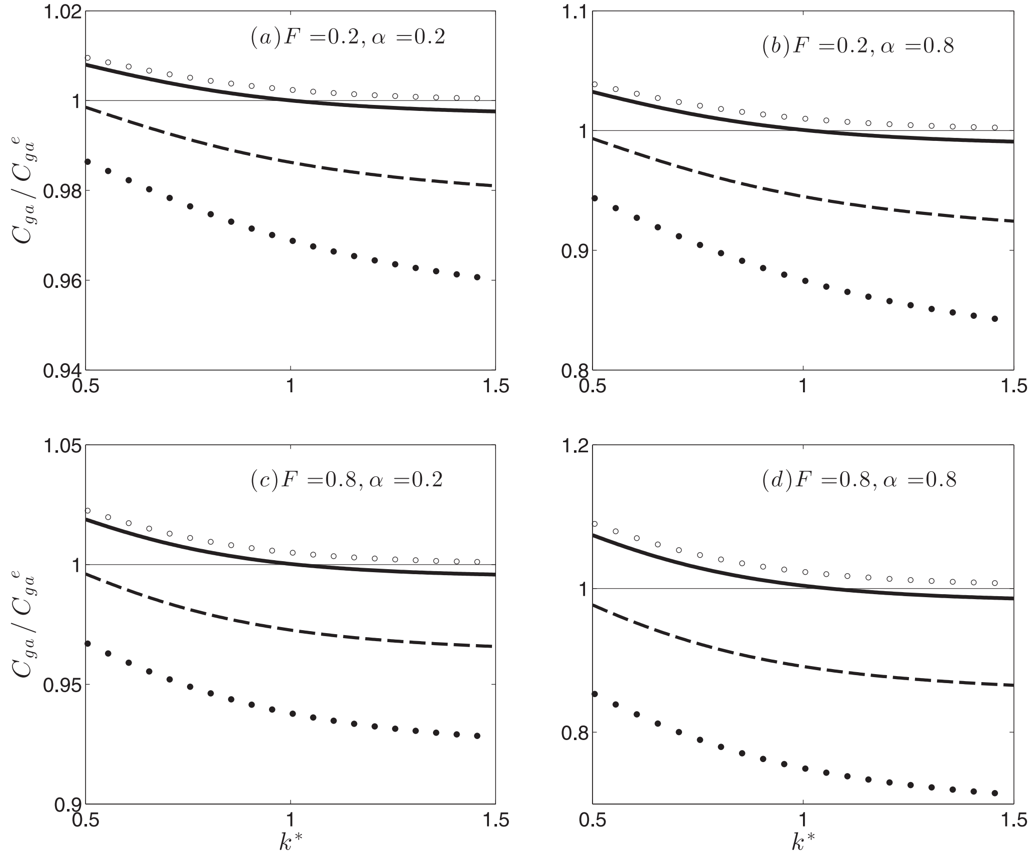

Fig. 11. Wave group velocity comparison C_{ga}/C_{ga}^e vs normalized wave number $k^* = k/k_p$, with $k_p h = 2$: linear shear flow. Solid lines are using $\hat{U}(k_p)$, dashed lines are based on $\tilde{U}(k_p)$, dots indicate the depth averaged approximation and the circles are only using the surface value U_s.

as

$$\hat{U}(k_p) = \tilde{U}(k_p) + k_p \frac{\partial \tilde{U}}{\partial k}\bigg|_{k_p} \tag{45}$$

For the linear shear case, the Taylor series coefficients are given by

$$\begin{aligned} \frac{\partial \tilde{U}}{\partial k} &= \alpha \frac{U_s}{2} \frac{\mu}{k}(1 - G) \\ \frac{\partial^2 \tilde{U}}{\partial k^2} &= \alpha \frac{U_s}{2} \frac{\mu}{k^2}[G^2(\cosh 2kh - 1) + 2G - 2] \end{aligned} \tag{46}$$

For the numerical case, the first two derivatives of $\tilde{U}$ are obtained from (A.9).

Comparisons for both analytic and numerical cases are shown in Figs. 16–21, for three different cases of $k_p h = 1, 2$ and 3. Considering a narrow-banded spectrum in frequency or wave number, it is seen that the Taylor series approach provides a good estimate of the group velocity while including the first order correction to the group velocity, as explained in (12), and evaluating it for just one peak wavenumber shows rapid deviation from the exact solution. The Taylor series approximation could thus be used as the basis for estimating frequency-dependent current values, with the wave model being able to construct a reasonable estimate of the group velocity using a minimal set of additional information.

7. Discussion and conclusions

The main aims of the present work have been to emphasize that the depth-weighted current value $\tilde{U}$ in (1) is not the appropriate leading-order estimate for current velocity in expressions for group velocity, and that the use of velocity evaluated at peak frequency can lead to rapid accumulation of error at frequencies away from the peak. The first point has been demonstrated by showing that the retention of wavenumber dependence in $\tilde{U}$ when differentiating the approximate dispersion relation to obtain group velocity leads to results which are consistent with an exact solution in the case of waves on a current with constant shear, and with a numerical solution computed using a candidate, strongly sheared current profile from MCR.

In order to illustrate the effect of an incorrect choice of current on wave predictions, we end with an example of a shoaling calculation based monochromatic waves propagating in constant depth against an increasingly strong opposing flow. We take the MCR current profile shown in Fig. 7 as reference $U(x_m, z)$ and construct a current distribution

$$U(x, z) = U(x_m, z)\frac{x - x_0}{x_m - x_0} \tag{47}$$

where x_0 represents an offshore starting point and the wave shoals in the interval $x_0 \le x \le x_m$. Using wave action conservation for waves on a depth uniform current then gives a wave height distribution

$$\frac{H(x)}{H_0} = \sqrt{\frac{C_{g0}}{C_g(x)} \frac{\sigma(x)}{\sigma_0}} \tag{48}$$

where subscripts 0 denote initial values at x_0 and H is waveheight, with energy density $E = 1/8\rho g H^2$. Fig. 22 shows results for cases with C_g and σ evaluated using current values $\tilde{U}, \hat{U}, \overline{U}$ and U_s. The relative accuracy of the result based on $\hat{U}$ has been established in Section 4 and is used here as the reference for the three remaining choices. Results are shown for incident waves with periods ranging

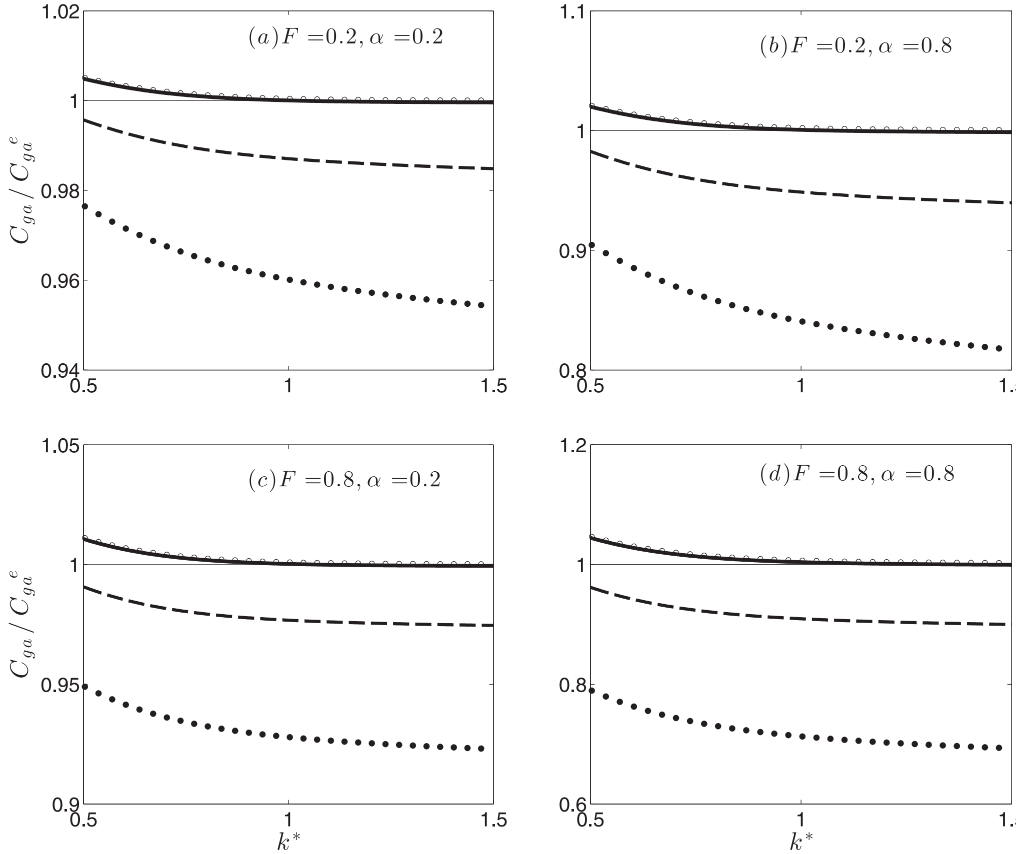

Fig. 12. Wave group velocity comparison $C_{ga}\ /C_{ga}^{e}$ vs normalized wave number $k^{*} = k/k_p$,with $k_p h = 3$: linear shear flow. Solid lines are using $\hat{U}(k_p)$, dashed lines are based on $\tilde{U}(k_p)$, dots indicate the depth averaged approximation and the circles are only using the surface value U_s.

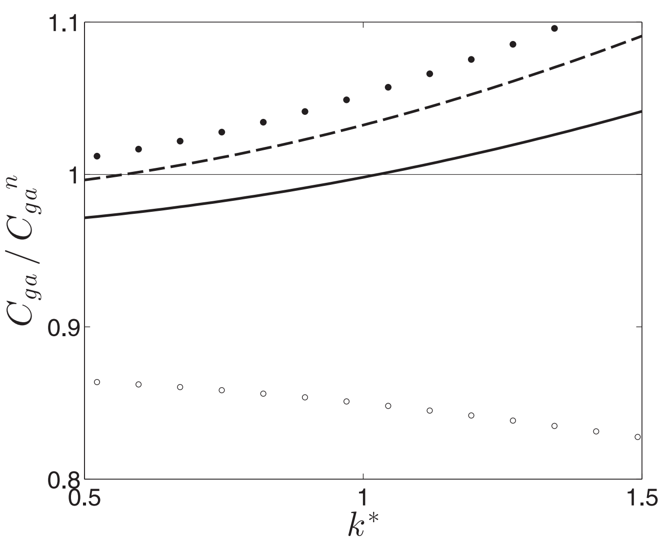

Fig. 13. Wave group velocity comparison $C_{ga}\ /C_{ga}^{n}$ vs normalized wave number $k^{*} = k/k_p$,with $k_p h = 1$: MCR velocity profile. Solid lines are using $\hat{U}(k_p)$, dashed lines are based on $\tilde{U}(k_p)$, dots indicate the depth averaged approximation and the circles are only using the surface value U_s.

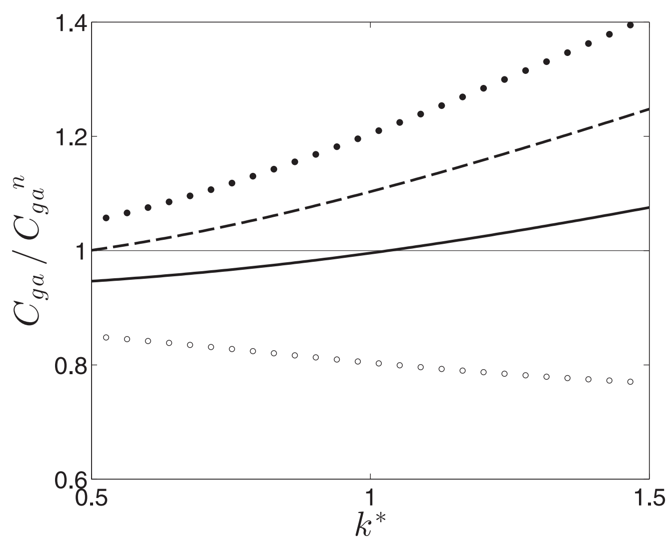

Fig. 14. Wave group velocity comparison $C_{ga}\ /C_{ga}^{n}$ vs normalized wave number $k^{*} = k/k_p$,with $k_p h = 2$: MCR velocity profile. Solid lines are using $\hat{U}(k_p)$, dashed lines are based on $\tilde{U}(k_p)$, dots indicate the depth averaged approximation and the circles are only using the surface value U_s.

from 6 to 12 seconds. As would be expected, the prediction based on $\hat{U}$ deviates the most from the value based on depth-averaged current $\overline{U}$ for shorter waves, where the influence of the larger currents near the surface is enhanced, and from the value based on surface current U_s the most for longer waves, where the weighting over depth becomes more uniform. The prediction based on $\tilde{U}$ is always closer to the correct answer than predictions made using surface or depth-averaged values, but errors are still significant and can be corrected using the proper expression $\hat{U}$.

The second point is cautionary in nature, and we have proposed a method for extending the range of model accuracy without imposing a massive increase in required data exchange between circulation and wave models.

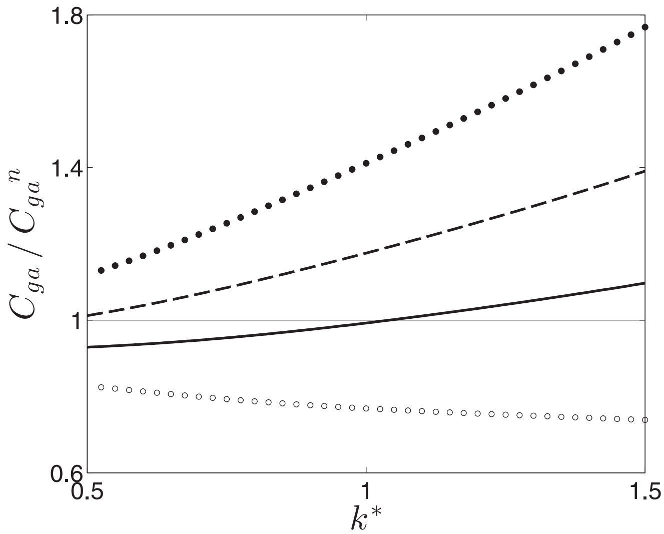

Fig. 15. Wave group velocity comparison C_{ga}/C^n_{ga} vs normalized wave number $k^* = k/k_p$, with $k_ph = 3$: MCR velocity profile. Solid lines are using $\hat{U}(k_p)$, dashed lines are based on $\tilde{U}(k_p)$, dots indicate the depth averaged approximation and the circles are only using the surface value U_s.

The results here are limited to an examination of the group velocity C_{ga} and do not address the corresponding approximations for wave action density. In particular, it is important to determine whether the action density can be approximated using a simple form $N = E_0/\sigma^*$, with $E_0 = 1/2\rho ga^2$ based on depth-uniform currents and $\sigma^* = \omega - kU^*$ with U^* related to the available weighted forms of U in some simple manner. (This problem has also been recently considered by Quinn et al., 2017). The theory described in this study is limited to unidirectional propagation on a following or opposing current, and so currents and wave numbers appear as scalars rather than vectors. The expressions for depth-weighted currents given here need to be extended to two horizontal dimensions for use in modeling, and the Taylor series expansion about peak wavenumber similarly needs to be developed in full vector form. These extensions are presently being developed and utilized in an extension of the SWAN wave model, and will be reported separately in the context of the description of a coupled system based on SWAN and the non-hydrostatic model NHWAVE (Ma et al., 2012). The break-down of the perturbation approach in the application to blocking of long waves requires further attention as well, and will be considered separately.

Acknowledgments

This work was supported by the National Science Foundation, Physical Oceanography Program grant OCE-1334325. MCR current data was extracted from file cr04008_30s_avg_small.mat, downloaded from http://makani.coas.oregonstate.edu/rise/data/adcp/june04_polemounted/.

Appendix A. Depth-weighted current velocities based on polynomial form of *U*(*z*)

We define the ambient current profile $U(z)$ in polynomial form as

$$U(z) = U_s \sum_{n=0}^{N} a_n \left(\frac{z}{h}\right)^n \tag{A.1}$$

where the a_n are defined by fitting to measurements or to grid-based numerical values. Evaluating $\tilde{U}$ from (1) then gives

$$\begin{aligned}\tilde{U} &= \frac{U_s G}{h} \sum_{n=0}^{N} a_n \int_{-h}^{0} \left(\frac{z}{h}\right)^n \cosh[2k(h+z)]\, dz \\ &= \frac{U_s}{h} \sum_{n=0}^{N} \frac{a_n}{h^n} J_n \end{aligned} \tag{A.2}$$

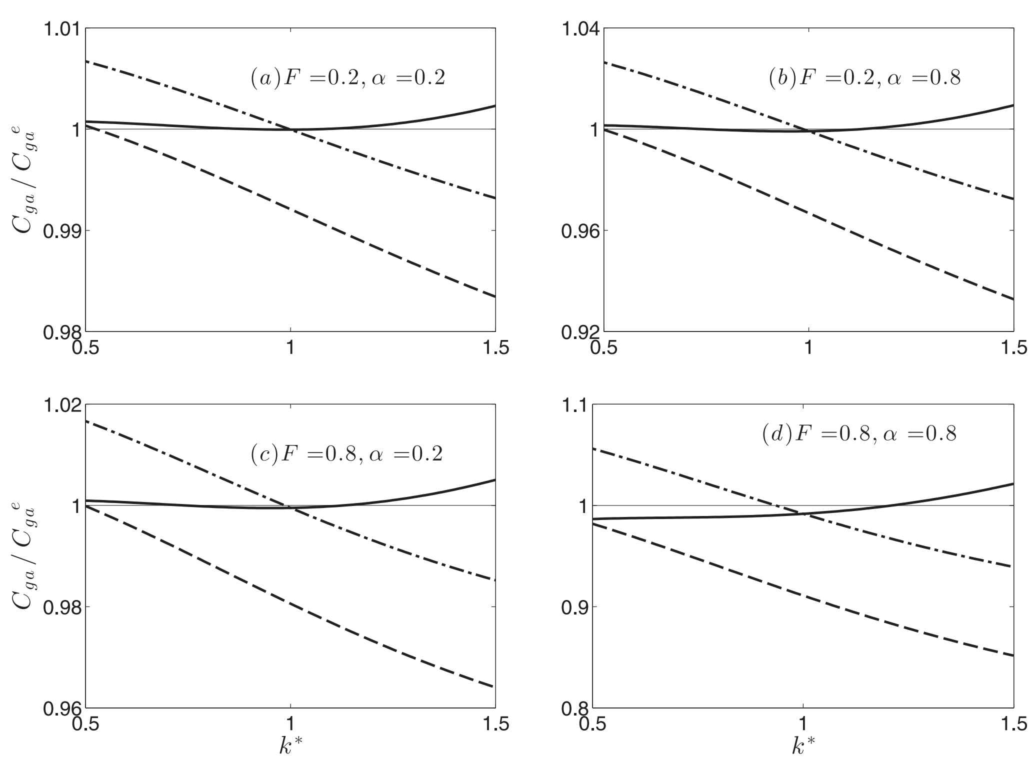

Fig. 16. Comparison of absolute group velocity C_{ga}/C^e_{ga} vs normalized wave number $k^* = k/k_p$,with $k_ph = 1$: linear shear flow. Solid lines are based on the Taylor series expansion of $\hat{U}(k)$ about k_p, dashed-dotted lines are based on $\hat{U}(k_p)$ and dashed line is using $\tilde{U}(k_p)$.

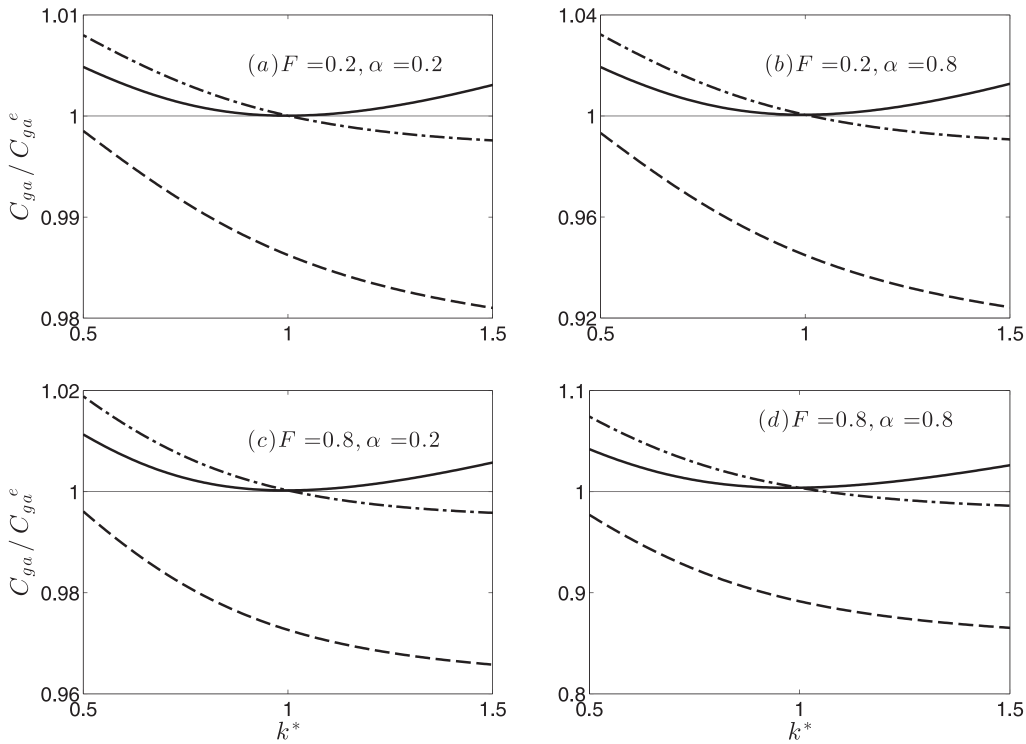

Fig. 17. Comparison of absolute group velocity C_{ga}/C_{ga}^e vs normalized wave number $k^* = k/k_p$, with $k_p h = 2$: linear shear flow. Solid lines are based on the Taylor series expansion of $\hat{U}(k)$ about k_p, dashed-dotted lines are based on $\hat{U}(k_p)$ and dashed line is using $\tilde{U}(k_p)$.

with J_n given by

$$J_n = G\int_{-h}^{0} z^n \cosh[2k(h+z)]\,dz \tag{A.3}$$

The first two terms J_0 and J_1 may be simply evaluated, after which the remaining J_n's are defined by a recurrence relation:

$$\begin{aligned} J_0 &= h \\ J_1 &= -\frac{h^2\mu}{2} \\ J_n &= \frac{n}{4k^2}\left[G(-h)^{(n-1)} + (n-1)J_{n-2}\right] \end{aligned} \tag{A.4}$$

For the polynomial of order $N = 6$ used in Section 5, $\tilde{U}$ is given by

$$\begin{aligned} \tilde{U} = U_s\Bigg[& a_0 - \frac{\mu}{2}a_1 + \frac{(1-G)}{2(kh)^2}a_2 + \frac{3(G-\mu)}{4(kh)^2}a_3 \\ & + \left(\frac{3(1-G)}{2(kh)^4} - \frac{G}{(kh)^2}\right)a_4 + \left(\frac{15(G-\mu)}{4(kh)^4} + \frac{5G}{4(kh)^2}\right)a_5 \\ & + \left(\frac{45(1-G)}{4(kh)^6} - \frac{15G}{2(kh)^4} - \frac{3G}{2(kh)^2}\right)a_6\Bigg] \end{aligned} \tag{A.5}$$

The derivative of $\tilde{U}$ w/r k is given by

$$\tilde{U}_k = \frac{U_s}{h}\sum_{n=0}^{N}\frac{a_n}{h^n}(J_n)_k \tag{A.6}$$

where subscript k denotes the derivative, and where $(J_n)_k$ can be expressed as

$$\begin{aligned} (J_0)_k &= 0 \\ (J_1)_k &= -\frac{h^2}{2}\mu_k \\ (J_n)_k &= \frac{-2J_n}{k} + \frac{n}{4k^2}\left[(-h)^{n-1}G_k + (n-1)(J_{n-2})_k\right] \end{aligned} \tag{A.7}$$

with

$$\begin{aligned} \mu_k &= \frac{\mu}{k}(G-1) \\ G_k &= \frac{G}{k}(1 - G\cosh 2kh) \end{aligned} \tag{A.8}$$

For $N = 6$, using (A.6) results in

$$\begin{aligned} k\tilde{U}_k = U_s\Bigg[& -\frac{k}{2}\mu_k a_1 - \frac{(kG_k - 2G + 2)}{2(kh)^2}a_2 + \frac{3(k(G_k - \mu_k) - 2(G-\mu))}{4(kh)^2}a_3 \\ & + \frac{-k(2h^2k^2+3)G_k + 4\,G(h^2k^2+3) - 12)}{2(kh)^4}a_4 \\ & + \frac{5(h^2k^3G_k + 3kG_k - 2\,G(h^2k^2+6) - 3k\mu_k + 12\mu)}{4(kh)^4}a_5 \\ & + \frac{-k(2h^4k^4 + 10h^2k^2 + 15)G_k + G(4h^4k^4 + 40h^2k^2 + 90) - 90)}{4(kh)^6}a_6\Bigg] \end{aligned} \tag{A.9}$$

The resulting $O(F)$ correction to the group velocity is finally given by

$$\hat{U} = \frac{U_s}{h}\sum_{n=1}^{N}\frac{a_n}{h^n}(kJ_n)_k \tag{A.10}$$

At $O(F^2)$, the expression for C_2 is given by (10), and can be written as

$$C_2 = \frac{\tilde{U}}{2C_0}A + \frac{k^2C_0}{2gf_0^2(0)}B + \frac{2k^3C_0}{gf_0^2(0)}C \tag{A.11}$$

where

$$\begin{aligned} A &= [4kI_1(0) - (1 + 2\cosh 2kh)\tilde{U}] \\ B &= \int_{-h}^{0} U^2(z)[1 + 2\cosh^2 k(h+z)]\,dz \\ C &= \int_{-h}^{0} [I_2(z)I_1'(z) - I_1(z)I_2'(z)]\,dz \end{aligned} \tag{A.12}$$

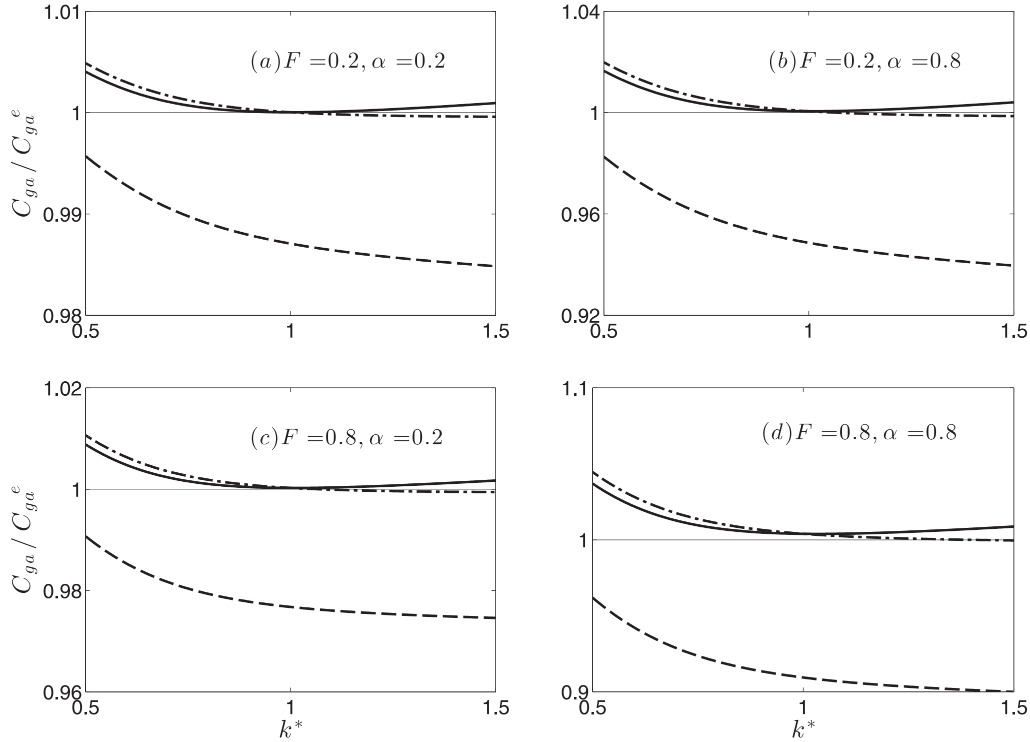

Fig. 18. Comparison of absolute group velocity $C_{ga}\,/\,C_{ga}^{e}$ vs normalized wave number $k^* = k/k_p$, with $k_p h = 3$: linear shear flow. Solid lines are based on the Taylor series expansion of $\hat{U}(k)$ about k_p, dashed-dotted lines are based on $\hat{U}(k_p)$ and dashed line is using $\tilde{U}(k_p)$.

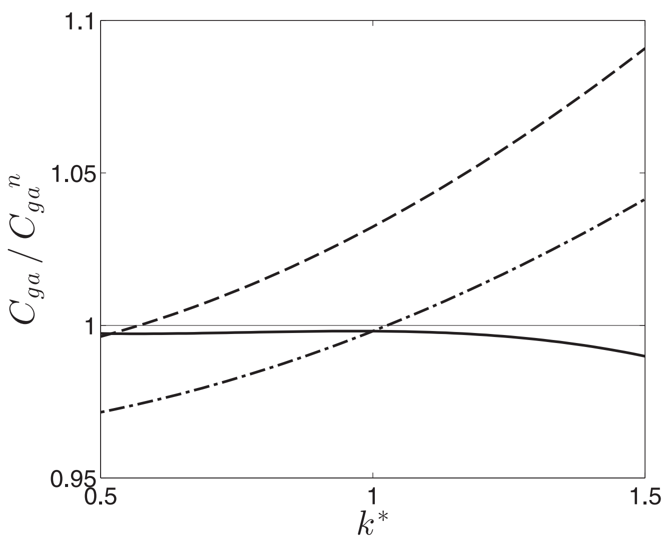

Fig. 19. Comparison of absolute group velocity $C_{ga}\,/\,C_{ga}^{n}$ vs normalized wave number $k^* = k/k_p$, with $k_p h = 1$: Mouth of Columbia River (MCR). Solid lines are based on the Taylor series expansion of $\hat{U}(k)$ about k_p, dashed-dotted lines are based on $\hat{U}(k_p)$ and dashed line is using $\tilde{U}(k_p)$.

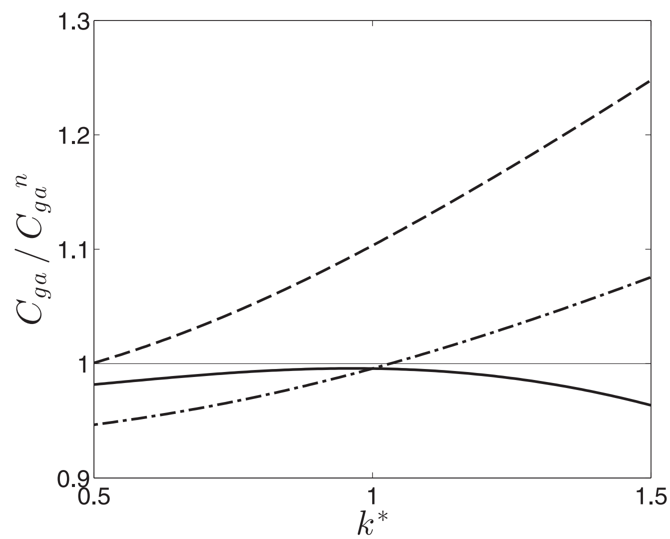

Fig. 20. Comparison of absolute group velocity $C_{ga}\,/\,C_{ga}^{n}$ vs normalized wave number $k^* = k/k_p$, with $k_p h = 2$: Mouth of Columbia River (MCR).Solid lines are based on the Taylor series expansion of $\hat{U}(k)$ about k_p, dashed-dotted lines are based on $\hat{U}(k_p)$ and dashed line is using $\tilde{U}(k_p)$.

with

$$I_1(z) = \int_{-h}^{z} U(\xi)\sinh 2k(h+\xi)\,d\xi$$
$$I_2(z) = \int_{-h}^{z} U(\xi)\cosh 2k(h+\xi)\,d\xi \tag{A.13}$$

We first evaluate the expressions for $I_1(z)$ and $I_2(z)$. Using the current profile (A.1), we obtain

$$I_1(z) = U_s \sum_{n=0}^{N} \frac{a_n}{h^n} \int_{-h}^{z} \xi^n \sinh 2k(h+\xi)\,dz$$
$$= U_s \sum_{n=0}^{N} \frac{a_n}{h^n} I_{1,n}(z) \tag{A.14}$$

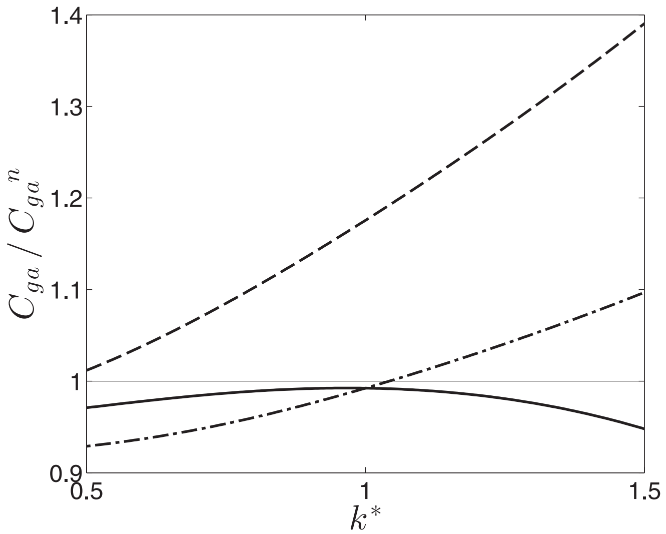

Fig. 21. Comparison of absolute group velocity C_{ga} / C_{ga}^n vs normalized wave number $k^* = k/k_p$, with $k_p h = 3$: Mouth of Columbia River (MCR). Solid lines are based on the Taylor series expansion of $\hat{U}(k)$ about k_p, dashed-dotted lines are based on $\hat{U}(k_p)$ and dashed line is using $\tilde{U}(k_p)$.

with

$$\begin{aligned}
I_{1,0}(z) &= \frac{\cosh 2k(h+z) - 1}{2k} \\
I_{1,1}(z) &= \left[\frac{z\cosh 2k(h+z) + h}{2k} - \frac{\sinh[2k(h+z)]}{4k^2}\right] \\
I_{1,n}(z) &= \frac{1}{4k^2}\big[2k(z^n \cosh 2k(h+z) - (-h)^n) - nz^{n-1}\sinh 2k(h+z) \\
&\quad + n(n-1)I_{1,n-2}\big]
\end{aligned} \tag{A.15}$$

Similarly, $I_2(z)$ can be expressed as

$$\begin{aligned}
I_2(z) &= U_s \sum_{n=0}^{N} \frac{a_n}{h^n} \int_{-h}^{z} \xi^n \cosh 2k(h+\xi)\, dz \\
&= U_s \sum_{n=0}^{N} \frac{a_n}{h^n} I_{2,n}(z)
\end{aligned} \tag{A.16}$$

with

$$\begin{aligned}
I_{2,0}(z) &= \frac{\sinh 2k(h+z)}{2k} \\
I_{2,1}(z) &= \left[\frac{z\sinh 2k(h+z)}{2k} - \frac{\cosh 2k(h+z) - 1}{4k^2}\right] \\
I_{2,n}(z) &= \frac{1}{4k^2}\big[2k(z^n \sinh 2k(h+z)) - nz^{n-1}\cosh 2k(h+z) \\
&\quad + n(-h)^{n-1} + n(n-1)I_{2,n-2}\big]
\end{aligned} \tag{A.17}$$

The expression A in (A.12) is evaluated using (A.14) and (A.16). Moving to the second term in (A.12), we have

$$\begin{aligned}
B &= \int_{-h}^{0} U^2(z)[1 + 2\cosh^2 k(h+z)]\, dz \\
&= \int_{-h}^{0} U^2(z)[2 + \cosh 2k(h+z)]\, dz \\
&= U_s{}^2 \sum_{n=0}^{N}\sum_{m=0}^{N} \frac{a_n a_m}{h^{n+m}} \int_{-h}^{0} z^{n+m}(2 + \cosh 2k(h+z))\, dz \\
&= U_s{}^2 \sum_{n=0}^{N}\sum_{m=0}^{N} a_n a_m \left[\frac{2h}{m+n+1}(-1)^{n+m+2} + \frac{1}{h^{n+m}} I_{2,n+m}(0)\right]
\end{aligned} \tag{A.18}$$

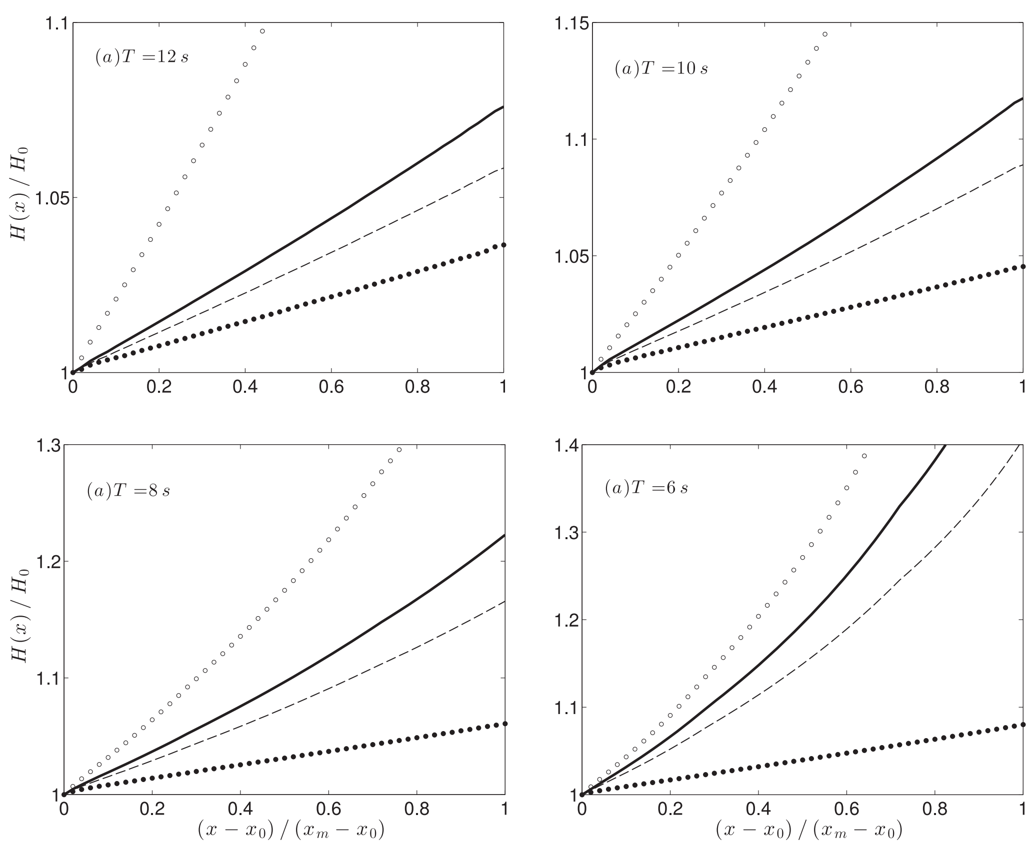

Fig. 22. Wave shoaling $H(x)/H_0$ for waves on an opposing current of the form shown in Fig. 7. Results are shown for four choices of current values, each used as a representation of depth-uniform current in determining wave action. $\hat{U}$: solid line; $\tilde{U}$: dashed line; $\overline{U}$: dots; U_s: circles.

The last term in (A.12) is given by

$$C = \int_{-h}^{0} [I_2(z)I_1'(z) - I_1(z)I_2'(z)]\,dz$$
$$I_1'(z) = U(z)\sinh 2k(h+z) \tag{A.19}$$
$$I_2'(z) = U(z)\cosh 2k(h+z)$$

and can be written as

$$C = U_s{}^2 \sum_{n=0}^{N}\sum_{m=0}^{N} \frac{a_n a_m}{h^{n+m}} H_{n,m} \tag{A.20}$$

with

$$H_{n,m} = \int_{-h}^{0} z^m [I_{2,n}(z)\sinh 2k(h+z) - I_{1,n}(z)\cosh 2k(h+z)]\,dz \tag{A.21}$$

For the polynomial form, $H_{n,\,m}$ is given by

$$H_{0,m} = \frac{1}{2k}\left[\frac{(-h)^{m+1}}{m+1} + I_{2,m}(0)\right]$$
$$H_{1,m} = \frac{1}{2k}\left[\frac{(-h)^{m+2}}{m+2} + (-h)I_{2,m}(0) + \frac{I_{1,m}(0)}{2k}\right] \tag{A.22}$$
$$H_{n,m} = \frac{1}{2k}\left[\frac{(-h)^{n+m+1}}{n+m+1} + (-h)^n I_{2,m}(0) + \frac{n(-h)^{n-1}}{2k} I_{1,m}(0) + \frac{n(n-1)}{2k} H_{n-2,m}\right]$$

The resulting second order correction to group velocity will be

$$C_{g2} = \frac{\partial kC_2}{\partial k} = C_2 + k\frac{\partial C_2}{\partial k}$$
$$= C_2 + k\left[\frac{\partial}{\partial k}\left(\frac{\tilde{U}}{2C_0}\right)A + \frac{\tilde{U}}{2C_0}A_k + \frac{\partial}{\partial k}\left(\frac{k^2C_0}{2gf_0^2(0)}\right)B + \frac{k^2C_0}{2gf_0^2(0)}B_k + \frac{\partial}{\partial k}\left(\frac{2k^3C_0}{gf_0^2(0)}\right)C + \frac{2k^3C_0}{gf_0^2(0)}C_k\right] \tag{A.23}$$

We also need an expression for $\tilde{U}_{kk}$ to be used in the Taylor series in Section 6. This is given by

$$\tilde{U}_{kk} = \frac{U_s}{h}\sum_{n=0}^{N}\frac{a_n}{h^n}(J_n)_{kk} \tag{A.24}$$

where $(J_n)_{kk}$ can be expressed as

$$(J_0)_{kk} = 0$$
$$(J_1)_{kk} = -\frac{h^2}{2}\mu_{kk} \tag{A.25}$$
$$(J_n)_{kk} = \frac{2J_n}{k^2} + \frac{-1}{2k^3}\left[n(-h)^{n-1}G_k + n(n-1)(J_{n-2})_k\right] - \frac{2(J_n)_k}{k} + \frac{1}{4k^2}\left[n(-h)^{n-1}G_{kk} + n(n-1)(J_{n-2})_{kk}\right]$$

with

$$\mu_{kk} = \frac{\mu}{k^2}\left[(G-1)^2 - (G-1) + G(1 - G\cosh 2kh)\right]$$
$$G_{kk} = \frac{G^2}{k^2}(G + G\cosh^2 2kh - 2\cosh 2kh) \tag{A.26}$$

A Matlab script which shows the evaluation of each of these expressions is provided as Supplement 1.

Supplementary material

Supplementary material associated with this article can be found, in the online version, at 10.1016/j.ocemod.2017.06.002

References

Ardhuin, F., Rascle, N., Belibassakis, K.A., 2008. Explicit wave-averaged primitive equations using a generalized lagrangian mean. Ocean Modell. 20, 35–60.

Constantin, A., 2011. Two-dimensionality of gravity water flows of constant nonzero vorticity beneath a surface wave train. European J. of Mech. B/Fluids 30, 12–16. doi:10.1016/j.euromechflu.2010.09.008.

Dong, Z., 2016. Wave-Current Interaction in Strongly Sheared Mean Flows. University of Delaware Ph.D. thesis.

Dong, Z., Kirby, J.T., 2012. Theoretical and numerical study of wave-current interaction in strongly-sheared flows. In: Lynett, P., Smith, J.M. (Eds.), Proceedings of the 33d Conference on Coastal Engineering. Santander, Spain.

Elias, E.P.L., Gelfenbaum, G., Van der Westhuysen, A.J., 2012. Validation of a coupled wave-flow model in a high-energy setting: the mouth of the Columbia river. J. Geophys. Res 117, C09011. doi:10.1029/2012JC008105.

Ellingsen, S.A., 2016. Oblique waves on a vertically sheared current are rotational. European J. of Mech. B/Fluids 56, 156–160. doi:10.1016/j.euromechflu.2015.11.002.

Fenton, J.D., 1973. Some results for surface gravity waves on shear flows. J. Inst. Math. Appl. 12 (1), 1–20.

Jonsson, I.G., 1990. Wave-current Interactions. In: Le Méhauté, B., Hanes, D.M. (Eds.), The Sea. Ocean Engineering Science, 9. John Wiley & Sons, Inc., pp. 65–120.

Karageorgis, P., 2012. Dispersion relation for water waves with non-constant vorticity. Euro. J. Mech. B/Fluids 34, 7–12. doi:10.1016/j.euromechflu.2012.03.008.

Kilcher, L.F., Nash, J.D., 2010. Structure and dynamics of the columbia river tidal plume front. J. Geophys. Res. 115, C05S90. doi:10.1029/2009JC006066.

Kirby, J.T., Chen, T., 1989. Surface waves on vertically sheared flows: approximate dispersion relations. J. Geophys. Res. 94, 1013–1027.

Kumar, N., Voulgaris, G., Warner, J.C., 2011. Implementation and modification of a three-dimensional radiation stress formulation for surf zone and rip-current applications. Coastal Eng. 58 (12), 1097–1117.

Kumar, N., Voulgaris, G., Warner, J.C., Olabarrieta, M., 2012. "Implementation of the vortex force formalism in the coupled ocean-atmosphere-wave-sediment transport (COAWST) modeling system for inner shelf and surf zone applications". Ocean Modell. 47, 65–95.

Lesser, G.R., 2009. An approach to medium-term coastal morphological modelling. UNESCO-IHE, Institute for Water Education.

Ma, G., Shi, F., Kirby, J.T., 2012. Shock-capturing non-hydrostatic model for fully dispersive surface wave processes. Ocean Modell. 43, 22–35.

Maïssa, P., Rousseaux, G., Stepanyants, Y., 2016. Wave blocking phenomenon of surface waves on a shear flow with constant vorticity. Phys. Fluids 28 (032102). doi:10.1063/1.4942116.

Peregrine, D.H., 1976. Interaction of water waves and currents. Adv. Appl. Mech. 16, 9–117.

Quinn, B.E., Toledo, Y., Shrira, V.I., 2017. Explicit wave action conservation for water waves on vertically sheared flows. Ocean Modell. 112, 33–47. doi:10.1016/j.ocemod.2017.03.003.

Shrira, V.I., 1993. Surface waves on shear currents: solution of the boundary-value problem. J. Fluid Mech. 252, 565–584.

Skop, R.A., 1987. Approximate dispersion relation for wave-current interactions. J. Waterway, Port, Coastal, and Ocean Eng. 113, 187–195.

Stewart, R.H., Joy, J.W., 1974. Hf radio measurements of surface currents. In: Deep Sea Research and Oceanographic Abstracts, 21, pp. 1039–1049.

Thomas, G., Klopman, G., 1997. Wave-current interactions in the near shore region. Int. Adv. Fluid Mech. 10, 255–319.

Thompson, P.D., 1949. The propagation of small surface disturbances through rotational flow. Ann. N. Y. Acad. Sci. 51, 463–474.

Voronovich, A.G., 1976. Propagation of internal and surface gravity waves in the approximation of geometrical optics. Izv. Atmos. Oceanic Phys. 12, 850–857.

Warner, J.C., Armstrong, B., He, R., Zambon, J.B., 2010. Development of a coupled ocean–atmosphere–wave–sediment transport (COAWST) modeling system. Ocean Modell. 35 (3), 230–244.

van der Westhuysen, A., Lesser, G., 2007. Evaluation and development of wave-current interaction in SWAN: activity 6.4 of SBW project Waddenzee. Technical Report. Deltares (WL).